Point clouds and surface analyses to detect anomalies

3c Point clouds and surface analyses to detect anomalies

Giulia Sammartano[1,2], Giacomo Patrucco[1], Stefano Perri[1], Antonia Spanò[1,2]

1 Politecnico di Torino, Department of Architecture and Design. LabG4CH - Laboratory of Geomatics for cultural Heritage. antonia.spano,giacomo.patrucco,stefano.perri,giulia.sammartano@polito.it

2 Politecnico di Torino, FULL – Future Urban Legacies Lab interdepartmental centre

After the current state and morphology of the building had been identified and the geometric principles at the base of the design and construction of the architectural elements and astonishing spaces of the Turin Exhibition Center had been investigated, another in-depth analysis was conducted concerning possible alterations.

The possible alteration or decay that geomatic techniques are able to investigate affects the shape of surfaces. They can be detected thanks to the very accurate, dense points clouds and digital surfaces. Most material decay can sometimes be recognized using high scale and high-resolution orthophotos. What is important to underline is that all the analyses can be conducted by relying on pieces of qualitative and quantitative evidence. Another important aspect to note is the comparison of data and results of interdisciplinary analyses; as the detection of anomalies involves a sphere that is sometimes very interpretative, the combination of different investigations is sought to find evidence and collaborations and comparisons of different techniques are, therefore, generally very useful.

In this paragraph we will analyze a series of investigations that were applied from the roofs to the foundations of the Nervi halls, passing through the thicknesses of the ferrocement roofs. The analysis methods used both consolidated and some rather complex strategies which generally attested to in-depth studies that exploited geomatic techniques.

The most innovative aspects of non-destructive investigation techniques to monitor structural health monitoring include the possibility of exploiting the in-depth 3D knowledge of the construction elements in Chapter 8, dedicated to the aspects of modeling. Especially interesting implications will also be presented, arising from the interdisciplinary integrations of the investigations to identify any alterations or anomalies.

3c.1 Alterations of the horizontal surfaces of the roofs.

Among the photogrammetric products, a significant role is played by DSM (Digital Surface Model), even though it a laser scanning survey can also be used. This is a matrix of points, in which each pixel assumes a certain size according to the scale of the survey and a precise position in the plane associated with Cartesian coordinates in a chosen reference system. Moreover, a specific code associated with each pixel expresses a distance from a chosen plane, generally a height if the reference plane is horizontal.

Since horizontal and vertical reference planes in architecture and construction are essential to identify any out-of-plumb vertical structures or subsidence, or other anomalies of floors and horizontal structures, it is very easy to identify the presence of shape alterations by calculating the DSM, the reference of which to horizontal or vertical planes is easy to control with the help of topographic techniques that enable Cartesian reference systems to be easily established.[1]

The UAV photogrammetric survey made it possible to calculate the DSM of the roofs and of the surroundings of the building complex. The visualization of the altimetric information according to color scales enabled each pixel to be checked both visually and analytically for any differences in level. Figures 3c 1.1 and 3c 1.2, respectively, show both the complete DSM panels of each roof of Halls B and C, and an enlarged extract enabled us to estimate the extent of the troughs in the roof slab, which create puddles of rainwater after rainfall.

The difference in height was approximately up to 13 cm for the coverage of Hall C and approximately up to 8 cm for the flat roof portion of the exedra of Hall B.

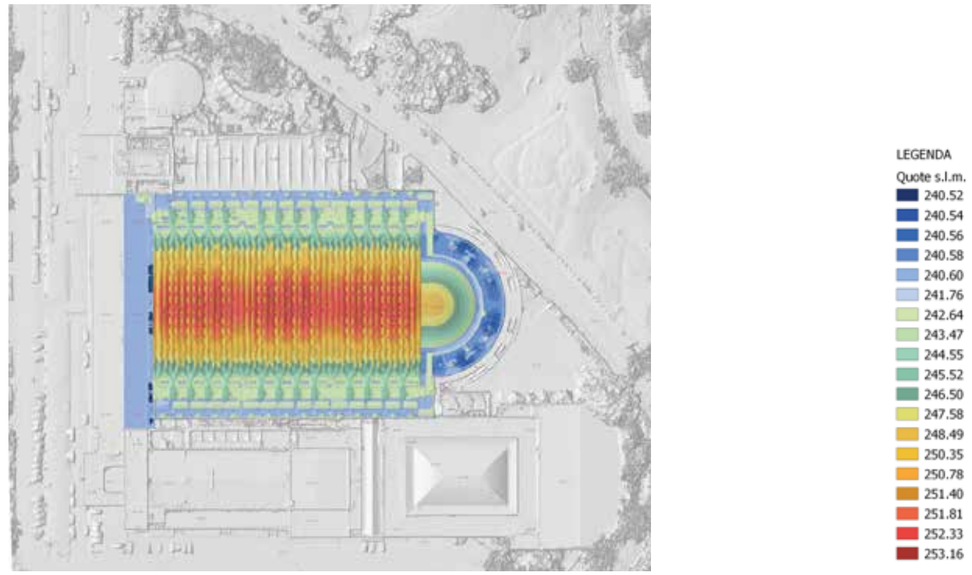

3c 1.1 (above): the DSM thematic view using range colors concerning the roof of Hall B, and (below) an extract.

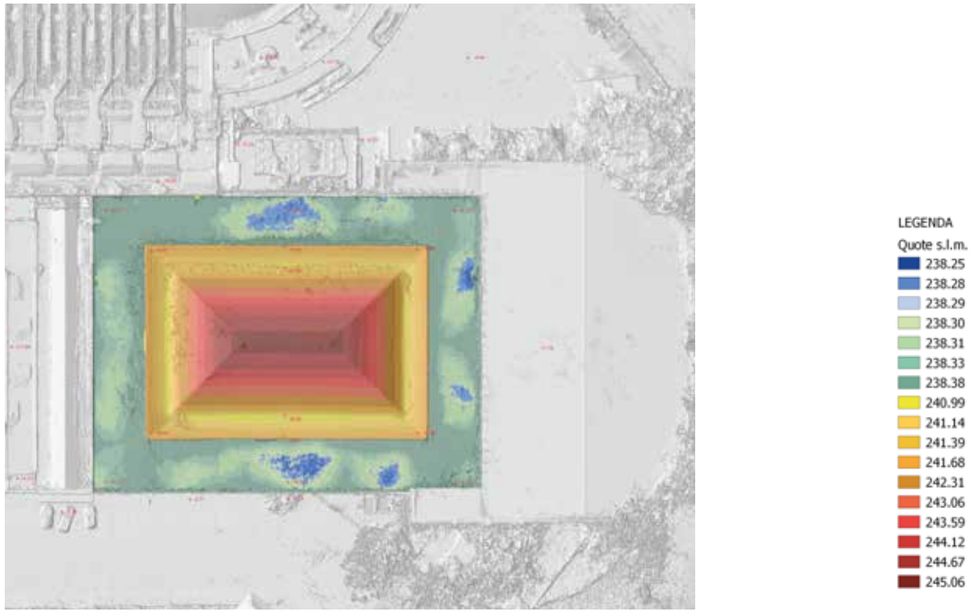

3c 1.2 (above): the DSM thematic view using a range of colors for the roof of Hall C, and (below) an extract.

1 Adamopoulos et al. 2017; Beltramo, Donadio & Spanò 2019, Barazzetti et al. 2015.

3c.2 Cracks in the ceiling of the basement of Hall B

The 3D survey of the basement of Hall C was rather complicated due to the absence of light, which made the use of photogrammetry problematic, even though the use of battery-powered lamps was tested. In essence, the very large spaces excluded the effectiveness of directed lights.

The use of the MMS system was also rather critical, as the regularity of the grid of the pillars combined with the reflective surfaces of the pipelines and the widespread puddles on the floor caused by water leaks, made the potential of the SLAM strategy rather ineffective and produced drifts in the calculation of the trajectory.

The handheld scanner obviously proved to be appropriate in the small rooms. However, the only effective technique in the large room below the apse area of Hall C was terrestrial laser scanning.

In addition to the usual distribution of the rooms and their different conformation, it was important to map a widespread system of cracks of different sizes in the basement, which certainly denoted a problem in the construction system with ceiling panels used in the construction.

The examination of the point cloud and especially of the triangulated surface (mesh) made it possible to estimate and map the presence of cracks that all ran parallel to the direction of the prefabricated, reinforced concrete panels (Figures 3c 2.1 and 3c 2.2).

3c 2.1: Two examples of cracks running along the longitudinal direction of reinforced concrete ceiling panels. To be clearly visible even simply in a photo, the light from the flash had to pinpoint the anomaly, hence the difficulty to use photogrammetry

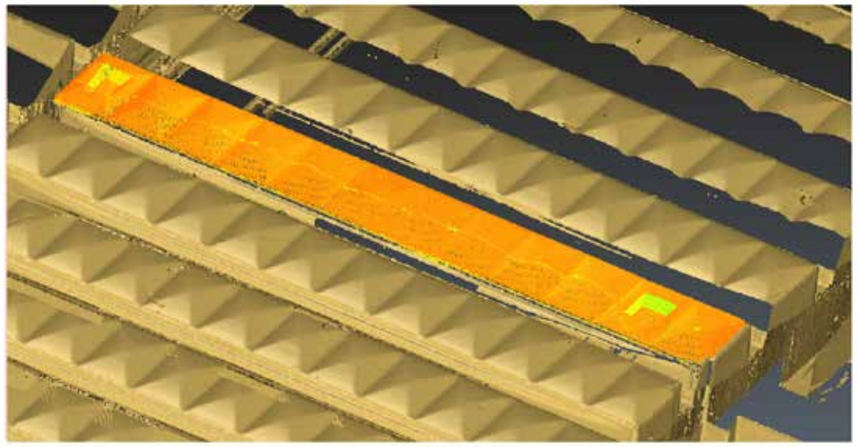

3c 2.2: A view of the triangulated surface (mesh) of a portion of the basement ceiling of Hall B; a portion of the cloud of points relating to a row of prefabricated panels was superimposed to better highlight the reading of the crack

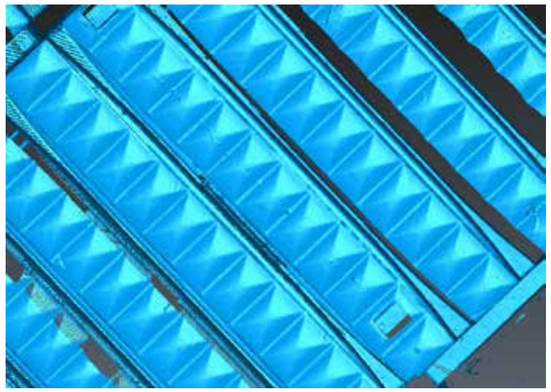

3c 2.3: Another view of the triangulated surface clearly shows a crack, which causes variations in the shape of the mesh

This clear reconnaissance of the basement mesh and the constant comparison with photos depicting the ceiling made it possible to map the entire crack pattern of the underground rooms. It was also decided that when a crack was so big it could be read on the cloud or on the mesh, i.e. of such a size as to cause a variation in the continuity of the surface acquired with the laser scanning technique, it was classified as main. If, on the other hand, the cracks were visible on the photo, but not on the surface, the lesion was interpreted as secondary, i.e. it substantially affects the plaster. Figure 3c 2.4 represents the final result of the mapping described above.

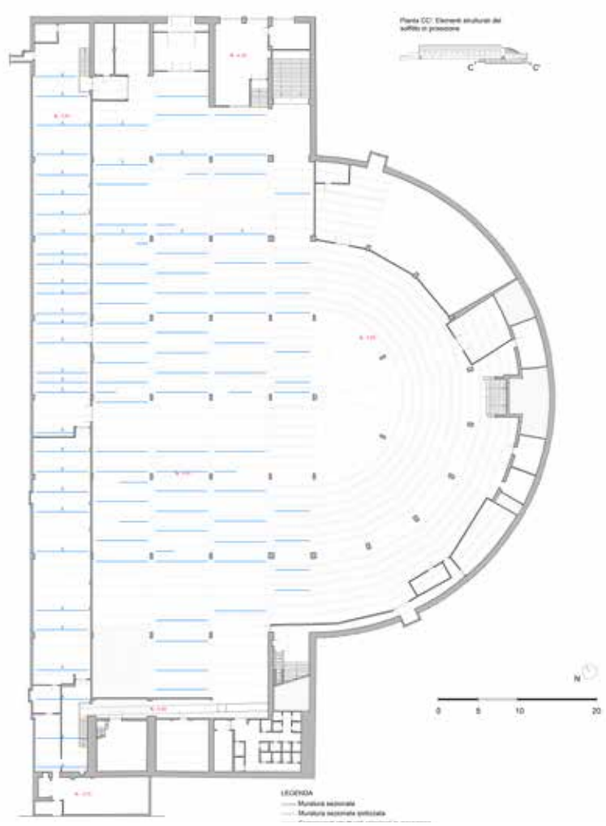

3c 2.4: Basement plan showing the map of the cracks detected both by the triangulated surface (main lesions) and by visual on-site inspection and with the support of photos (secondary lesions).

3c.3 The foundations and the grid of pillars of Hall C

Building foundations of buildings are not usually, or often only partially visible, so it is difficult for geomatic techniques, which typically deal with documenting visible forms and phenomena, to collaborate in studies on foundations.

All the drawings made from the 3D metric survey actually show and integrate the design of the foundations according to the Nervi project documented by the project drawings (CSAC, Università di Parma, courtesy Fondation PLN Project); as regards Hall B, since all the inclined pillars are an integral part of the architectural design of the room space, they are in full view and there is no doubt as to the location of the foundations (Figure 3c 3.1)

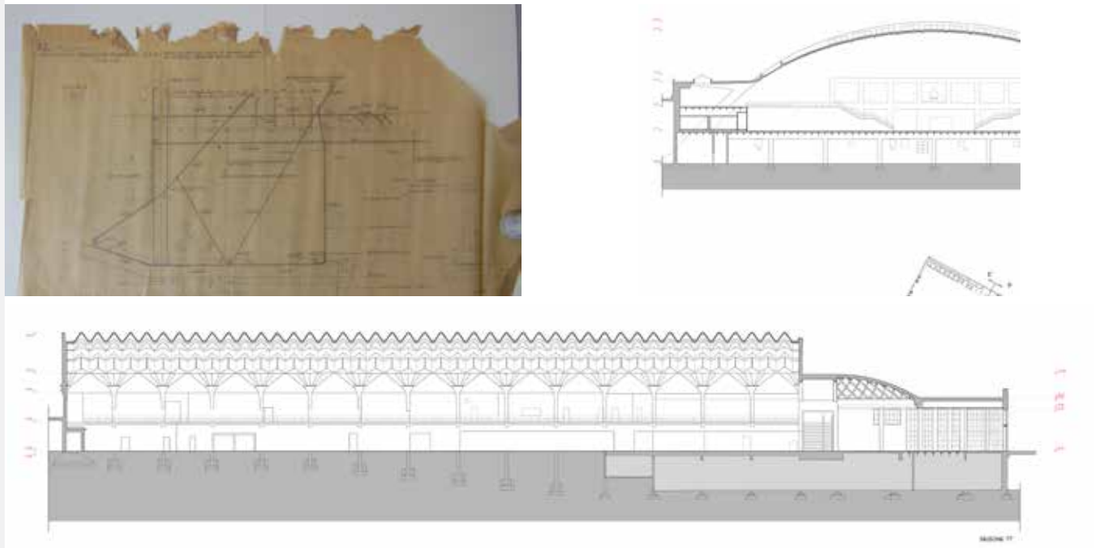

3c 3.1: Completion of the architectural drawings with the integration of the design of the foundations according to Pier Luigi Nervi's design drawings. (above, left) the foundation of an inclined pillar (CSAC, Università di Parma, courtesy Fondation PLN Project), (above right) an extract of Section EE ', (below) longitudinal section TT', performed not in the centre line.

In Hall C, the large arches that support the roof are, as is known, detached from the perimeter walls and the grid of the pillars within the surrounding walls has been the subject of interest, thanks to a general overview of more than a hundred thermograms acquired by A. Manuello and E. Lenticchia and reported in Chapter 5a 4.7 in Hall C. After visual observations, the Geomatics group began another focusing thermal survey and the results are reported in this paragraph.

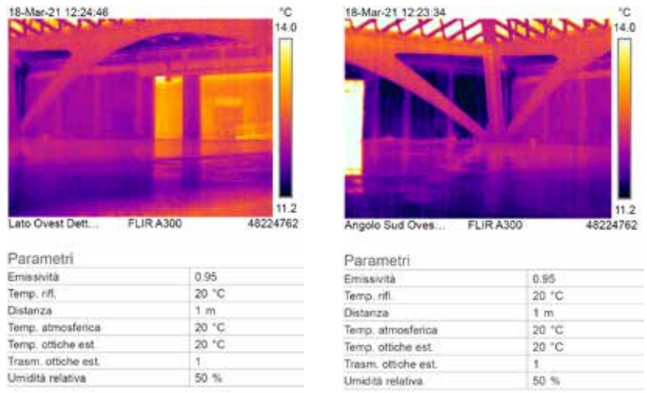

3c 3.2: Two examples of thermograms acquired by A. Manuello and E. Lenticchia and reported in Chapter 5a 4.7; the second image shows an anomaly, inthe height of the pilasters and the ring beam, which suggested the Geomatics group should conduct a more in-depth analysis.

The in-depth study began by analyzing the drawings of the Nervi foundations in Hall C.

As regards the drawings in Figure 3c 3.3, the foundations feature four large plinths positioned respectively at the four top corners of the hall. They are made of reinforced concrete and support the four arches of the hall. As regards the perimeter walls, the 40x30 cm section pillars disappear into the masonry and the angular pillars resting on the plinths that support the arches have a 40x40 cm cross-section.[2]

New vector drawings and the 3D model of the foundations were the term of reference for the new thermal survey.

A thermographic image corresponds to a raster map representing the variations in radiation intensity; a deep connection between infrared radiation and temperature exists according to the rule of black body radiation, which states that all objects emit infrared radiation based on their temperatures.[3]

In the framework of geomatic techniques, it is possible to stress that the current potential of the combined use of visible and thermal data in the framework of photogrammetric processing using semi-automatic techniques for image orientation, is demonstrated by the fact that many SfM photogrammetric software developers (both commercial and open-source) have implemented new algorithms and specific templates in order to allow thermal images to be managed and processed.[4]

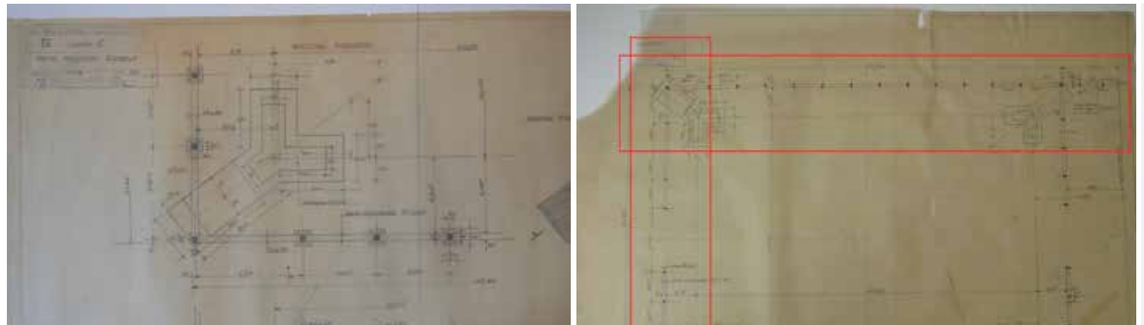

3c 3.3: Plan of the foundations of Hall C, and (above) a detail of the foundation plinth positioned at the corners of the room.

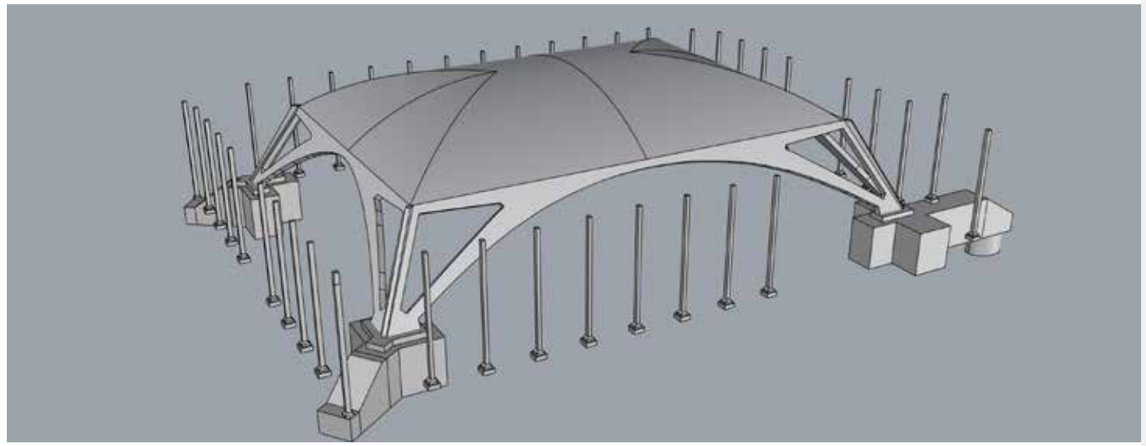

3c 3.4: A 3D model generated from Nervi's drawing, focusing on the main structural elements of Hall C (foundations, pillars, arches, and the vault.) (elab. Cofano)

2 It is interesting to notice that since these drawings were useful for Nervi to calculate the size of the reinforced concrete rods, the drawings are said to have a precision of half a millimeter.

3 Kuenzer & Dech 2013. Patrucco, Cortese, Giulio Tonolo, Spanò 2020.

4 Lerma et al. 2012, Patrucco et al. 2022.

The thermal conditions of the environment subject to thermal survey are often related to the time of day at which the acquisition of thermal images takes place. They are often crucial in order to obtain a high thermal contrast between the different construction materials and to optimize the view to interpret the buildings and identify any anomalies. In the this case, we can present, as a preliminary step, two drawings resulting from a mosaic of thermograms, which were previously assigned a reclassification to standardize the graphic scale for the variation in temperatures. The merge process of the thermal images was produced by means of a rigorous photogrammetric process to identify homologous points on the 3D model and determine the projection center of thermograms, which enabled a good mosaic to be obtained. (Figures 3c 3.5 - 3c 3.6)

.

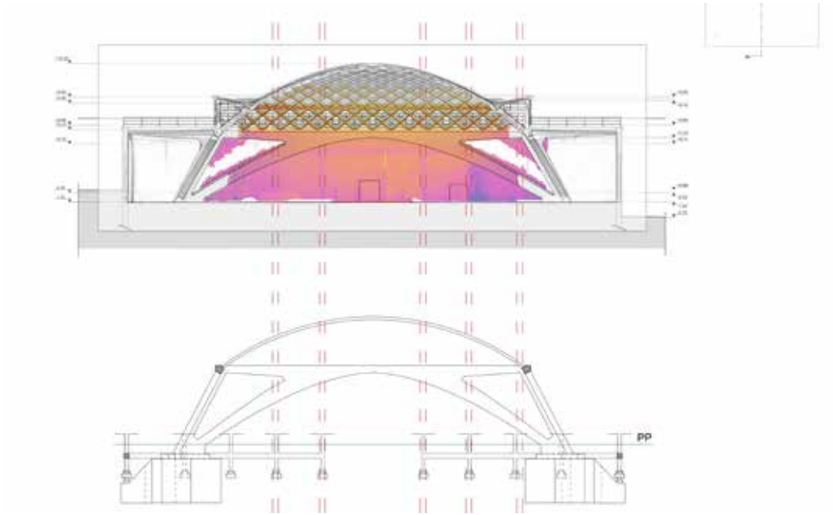

3c 3.5: Comparison between the position of pillars from the thermal survey and positions from Nervi's drawings for the east interior wall. (elab. Patucco, Cofano)

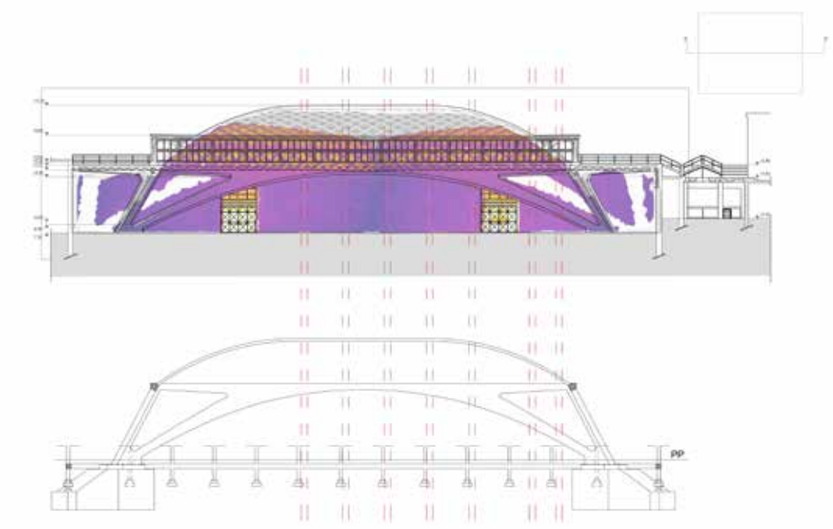

3c 3.6: Comparison between the position of pillars from the thermal survey and positions from Nervi's drawings for the south interior wall. (elab. Patucco, Cofano)

It can be clearly seen that something occurred to the pillars and foundation design in Hall C prior to the construction site. Whereas the correspondence between the pillars and the project foundations for the interior east front is very precise, a significant deviation can be observed for the interior south front. This is a sign that once again the plan of the foundations should not have been the definitive plan.

3c.4 Shape anomalies of the SAP vault in Hall B

The so-called SAP vault (reinforced concrete-brick vault) once again offered the opportunity to test the possibilities for analyzing and interpreting the overall architectural form of structural elements via the point cloud, based on its geometric contents.

The first two images (3D and nadiral view) of Figure 3c 4.1 show the point cloud transformed into a continuous surface (mesh) and the extraction of isohypses (contour lines referring to the land) at a distance of very few centimeters (10 cm). The altered shape of such lines can demonstrate the specified design geometry and the possible anomalies of shape. These can also be in the form of asymmetries of spatial configuration which, when compared with other structural investigations, can provide important clues to formulate the presence of deformations, which have occurred after construction.

In this case, after we had ascertained the presence of a slope of the arch in the direction of the exedra, we made another assumption. Figure 3b 1.2. in paragraph 3b, highlighted that the apparent shape of the arch is a parabola, and the deviation from a circular cylinder is a few centimeters (3-4 cm) away from the nearby key and spring of the arch.

The final image in Figure 3c 4.1. shows we can investigate the problem further by comparing the measured point cloud and the ideal cylinder, which confirms a maximum deviation of 3.5 cm in the direction of the apse dome.

We are quite convinced that if everything in the previous reasoning is correct, the lowering is not to be ascribed to a slight subsidence or deformation after construction but rather to a more credible, skillful adaptation during construction, which took place using the accentuated principles of on-site prefabrication., Pier Luigi Nervi had to connect the cross-section of a cylinder with a parabolic cross-section with the cross-section of a sphere. (circular).

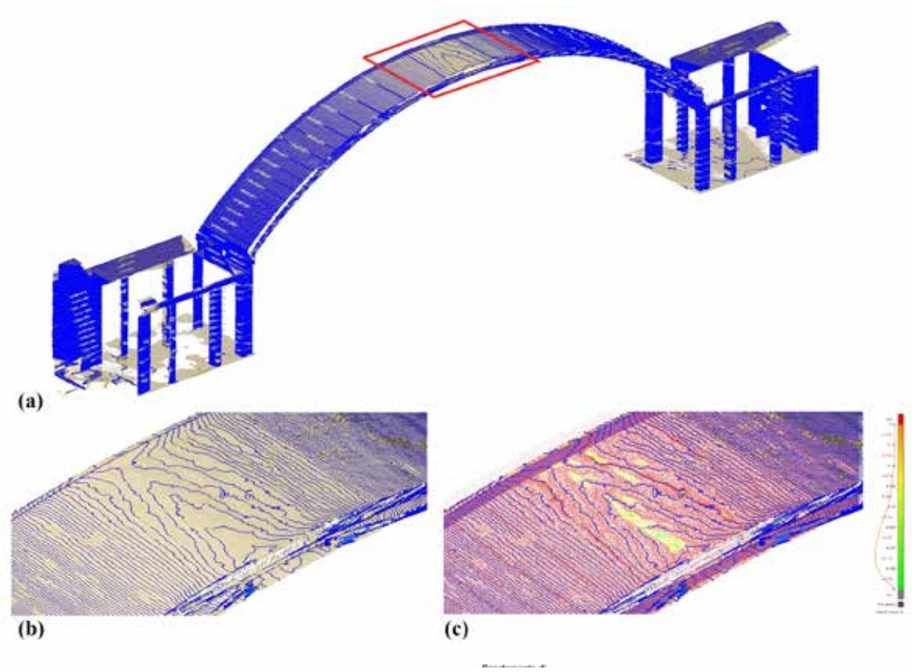

3c 4.1: Extraction of isohypses from the point cloud of the so-called SAP vault (above and below left), together with a pixel-to-pixel difference of surfaces showing a lowering of the arc in the direction of the dome.

3c.5 Morphology of the envelope shape via intrados/extrados integration and comparisons with historic design drawings. Halls C and B.

The morphological feature of the thin envelope was addressed, as illustrated in the previous paragraphs, by first integrating the data relating to the intrados (LiDAR scans) and the extrados (point cloud from UAV photogrammetry) of the structure.

Starting from Hall C, particular interest was dedicated to the possibility of verifying the correspondence of the ferrocement elements of the design phase with the actual construction, thanks to a reality-based model. To do this, the archive drawings relating to Hall C were analyzed and a correspondence was created with the real sections [figure 3c.5.3]. The expected thickness of the latter was 5cm, with the addition of a 2cm waterproof sheath. It was decided to verify this correspondence on the 3D model using a sample of 12 points distributed on the curvature of the envelope. The average value calculated from this sample of measurements was 7.4 cm, with a standard deviation of 1.2 cm. These values would prove to be perfectly consistent with Nervi's project. However, this thickness of the envelope, which cannot be verified empirically, was replaced by a further verification based on a direct measurement performed on the perimeter skylight, Figure 3c.5.4. This results in a residual 1 cm error from the 3D cloud with respect to the project drawing, Figure 3c.5.3.

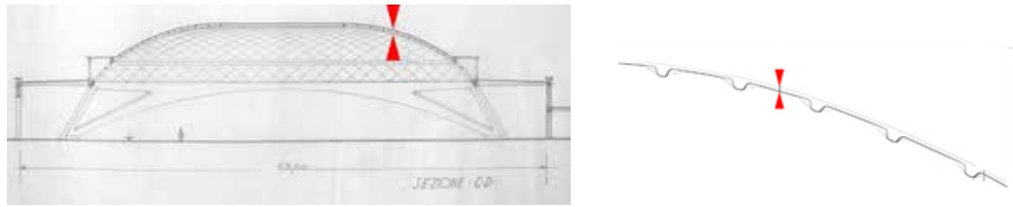

3c 5.1: Project drawing of the section of the vault of Hall C (CSAC, Università di Parma, courtesy Fondation PLN Project), and the corresponding intrados-extrados section on the integrated point model

3c 5.2: A view of the vaulted portion of Hall C without panels between the ribs to allow the hall to be illuminated.

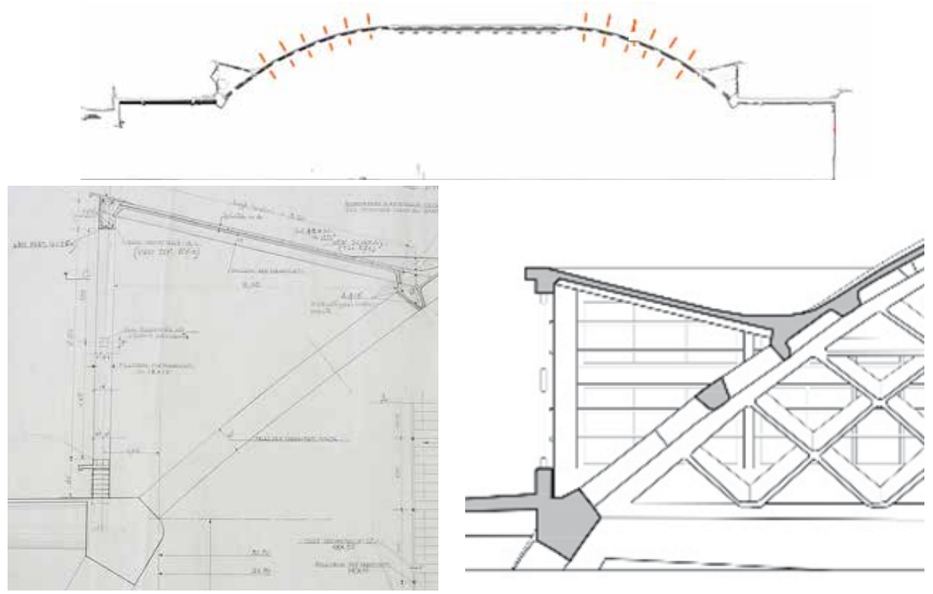

3c 5.3: Correspondence between sections of the reality-based point model and archive drawings (CSAC, Università di Parma, courtesy Fondation PLN Project). In orange, the 12 thickness measurement points were verified on the cloud, and in red the longitudinal verification was directed on the skylight of Hall C.

3c 5.4: A view of the same construction detail using the drawing with the overlapped orthophoto and a phase of the topographic measurement to assess the intrados-extrados relationship.

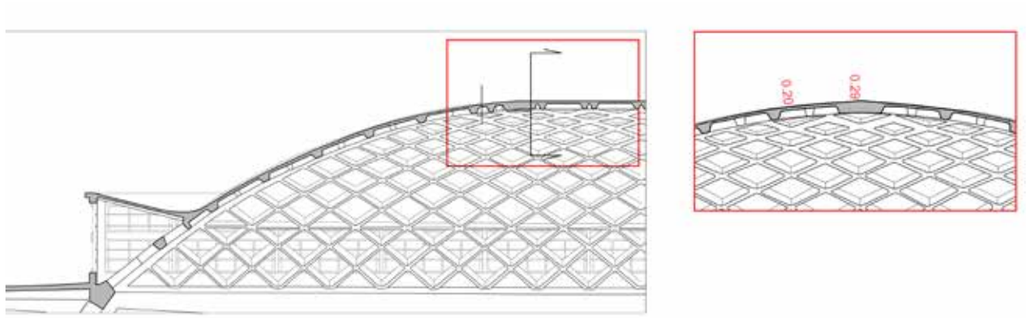

3c 5.5: A final drawing representing the dimensional relations between the envelope thickness and the ribs.

As regards the shape of the waves of the roof of Hall B, the measurement and verification operations were far more complicated (Figure 3c 5.6). First of all, we should point out, that the direction of the projecting rays appears to be useful for solving the photogrammetric problem from the aerial perspective of the UAV, the smooth surfaces of Hall C and the apse dome certainly offered surfaces with easier directions to reconstruct.

It should also be noted that the roof of the wave vault has a series of superstructures relating to the systems with reflective surfaces (pipelines and skylights), which are particularly critical for the photogrammetric technique based on visible spectrum images (Figure 3c 5.7).

We can add that the openings that allow light to enter Hall B are of two kinds: the first set has automatic opening mechanisms to air the room, whereas another series is fixed. The two configurations have different thicknesses, which makes it more difficult to calculate their thickness. (Figure 3c 5.8) Lastly, it is still useful to point out that walking on the surface of the bituminous sheath of the roof causes rainwater leaks that infiltrate inside the membrane.

All these reasons made the surface of the cloud detected by aerial photogrammetry particularly noisy with a thickness variability that was difficult to control.

3c 5.6: A view of the impressive shape of the parabolic-like waves of Hall B, with surfaces not oriented in favor of the incidence of the projecting rays of the photogrammetric blocks of images.

3c 5.7: Presence of a high quantity of systems and surfaces made of reflective materials in the roof of Hall B

3c 5.8: Different types of skylights in the roof of Hall B, with an automatic opening mechanism that requires a larger frame and fixed openings

In essence, the strategy adopted to determine the envelope of the undulated thin-shell vault of Hall B was as follows: a targeted photogrammetric process of the aerial block of images was re-performed, using only the images pertaining to the coverage of Hall B and an attempt was made to optimize the results in relation to noise and residual errors on the control points. In the light of this result, careful extraction of the average surface was carried out along the entire extension of the extrados of the undulated vault.

Subsequently, the portion detected by close-range photogrammetry using images acquired from close range through the elevator was selected as the sample surface (Figure 3c 5.9). This careful combination of medium surfaces led to the vectorization of the sections of the large, vaulted structure shown in the panels of the architectural drawings (Figures 3c 5.10)

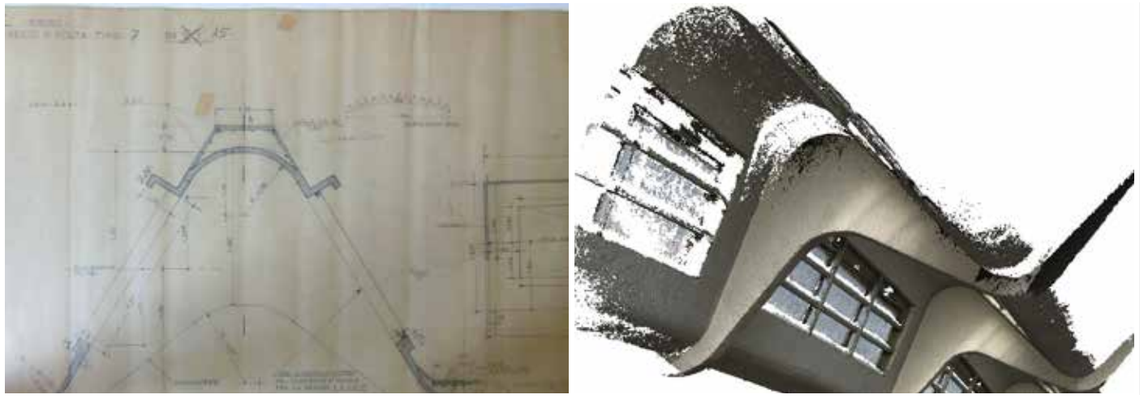

3c 5.9. (left): An in-depth study of the wave element of the Hall B vault in a very detailed drawing by Pier Luigi Nervi (CSAC, Università di Parma, courtesy Fondation PLN Project); (right) a view of the point cloud derived from close range photogrammetry of the same constructive element.

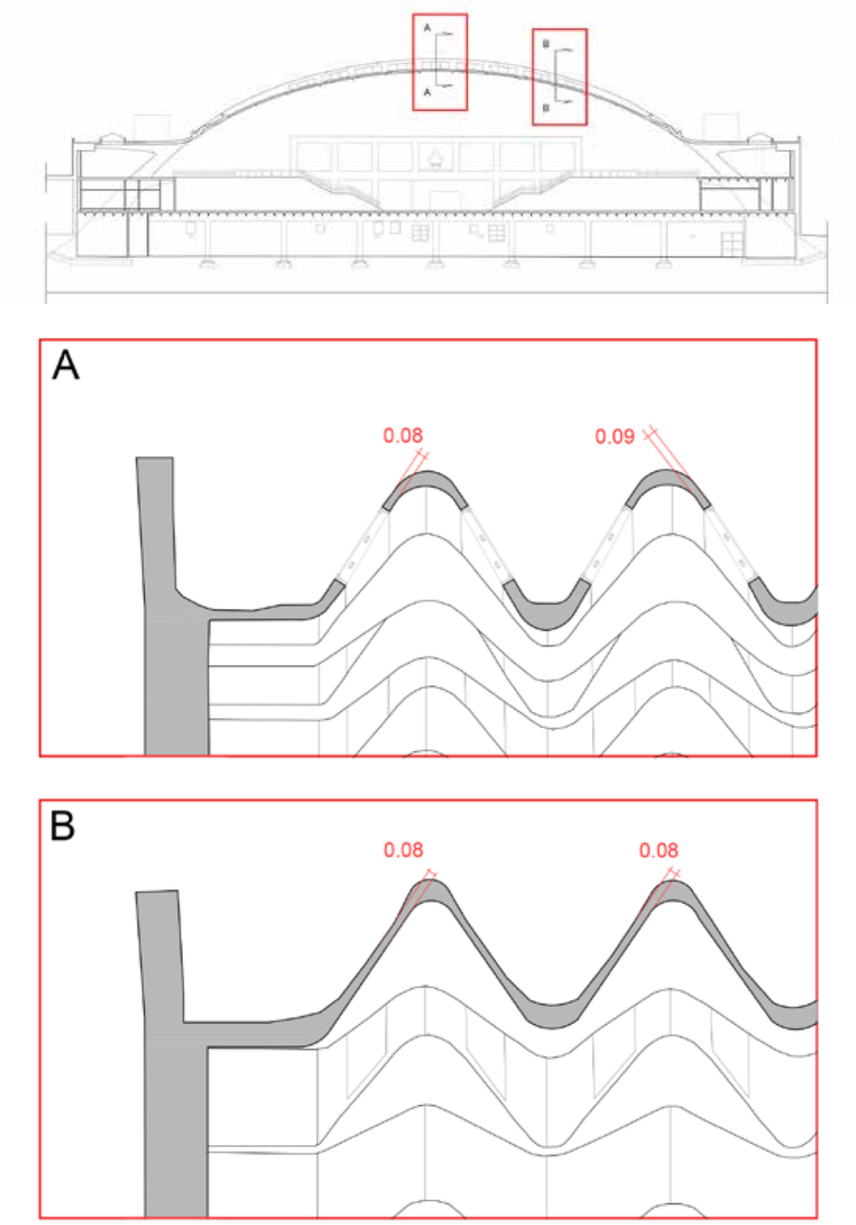

3c 5.10: Studies to calculate the thicknesses of the envelope of the vault of Hall B, and related architectural drawings in cross-section.